K-Shell Ionization of Rare Earth Elements in the Energy Range of 3-40 MeV/amu

I. 11. K-Shell Ionization of Rare Earth Elements in the Energy Range of 3-40 MeV/amu

*Sera K., Ishii K., Orihara H. and Morita S.**

Cyclotron and Radioisotope Center, Tohoku University
*Research Center of Ion Beam Technology, Hosei University**

We report here K-X ray production cross sections of Dy, Er and Lu by proton and ^{3}He-ion impact over the energy range of 3-40 MeV/amu, and compare the experimental results with the theoretical predictions.

Dy, Er and Lu metal targets were prepared by vacuum evaporation onto 1.5 μm-thick Mylar foils. Target thicknesses were determined by comparison of K-X ray yields with those from targets of known thicknesses. They are 169.8 μg/cm^2, 187.2 μg/cm^2 and 60.4 μg/cm^2 for Dy, Er and Lu respectively. Protons of 3, 6, 9, 15, 21, 30 and 40 MeV and ^{3}He-ions of 9, 18, 27, 45 and 63 MeV were accelerated by the AVF cyclotron of CYRIC. K-X rays produced by these projectiles were measured with an ORTEC Si(Li) detector. In front of the detector window, the 0.4 mm-thick Al absorber was put to reduce numerous M- and L-X rays.

Figure 1 shows the K-X ray spectrum of Er produced by 30 MeV proton impact. In this spectrum, at the high energy side of $K\alpha_2$ and $K\alpha_1$ lines, two peaks (x2, x1) can be recognized. These peaks always exist independent of target atom and projectile energy. The intensity ratios x1/$K\alpha_1$ and x2/$K\alpha_2$ are almost the same. Energy differences x1-$K\alpha_1$ and x2-$K\alpha_2$ slightly dependent on atomic number; ~1.40 keV for Dy, ~1.52 keV for Er and 1.65 keV for Lu, while they don't depend on projectiles and their energy. Intensity ratio x1/$K\alpha_1$ seems to depend on projectiles and their energy; 0.08~1.70 for protons and 0.03~0.05 for ^{3}He-ions. These peaks x1 and x2 might attribute to an interference between X ray signals and huge signals due to scattered ions from the target. In this work, the yields of peaks x1 and x2 are not included in the calculation of X ray production cross sections. (If x1 and x2 belong to $K\alpha_1$ and $K\alpha_2$, the experimental values become 3-17 % larger.) The experimental X ray production cross sections were obtained by the same way as has previously been reported.[1,2)]

Figures 2-5 show the experimental and the theoretical X ray production cross sections. Errors are mainly from target thickness (5 %), solid angle (5 %), detection efficiency (5-13

%) and fitting (1-10 %). The theoretical predictions are the PWBA[3], the ECPSSR[4] and the PSSR, where the values of Ref. 5) and 6) are used as fluorescence yields and radiative widths. The ECPSSR[4] includes the corrections for energy loss (E), Coulomb deflection (C), polarization and binding energy effects in the perturbed stationary state (PSS) and relativistic (R) effect of inner-shell electrons. As seen in these figures, experimental results are in excellent agreements with the ECPSSR over 3-40 MeV/amu energy range, while there is a systematic deviation from the PWBA. Especially, the discrepancy between experimental results and the PWBA becomes larger in lower incident energy region. Energy loss, Coulomb deflection and binding energy effects decrease ionization cross section, while relativistic effect increase it. In the present incident energy region, therefore, relativistic effect is the most predominant among these effects. Figures 5a-c show total K-X ray production cross sections for proton impact. The difference between the ECPSSR and the PSSR means the contribution of energy loss (E) and Coulomb deflection (C) effects, since the PSSR doesn't include them. It is seen in these figures that energy loss and Coulomb deflection effects become effective with the decrease of incident energy. The present experimental values of K-X ray production cross sections are tabulated in Table 1.

References

1) Sera K., Ishii K., Orihara H. and Morita S., CYRIC Annual Report (1986).
2) Sera K., Ishii K., Orihara H. and Morita S., CYRIC Annual Report (1987).
3) Merzbacher E. and Lewis H. W., Handb. Phys. **34** (1958) 166.
4) Brandt W. and Lapicki G., Phys. Rev. A **23** (1981) 1717.
5) Bambynek W., Crasemann B., Fink R. W., et al., Rev. of Mod. Phys. **44** (1972) 716.
6) Scofield J. H., Phys. Rev. A **10** (1974) 1507.

Table 1. K-X ray production cross sections for $K\alpha_2$, $K\alpha_1$, $K\beta_1$, and $K\beta_2$ lines (in barn).

	Projectile		$K\alpha_2$	$K\alpha_1$	$K\beta_1$	$K\beta_2$
Dy	p	3 MeV	0.0302±15%	0.0491±15%	0.0137±20%	0.00311±40%
		6	0.200 ±15%	0.367 ±15%	0.132 ±18%	0.0202 ±38%
		9	0.616 ±15%	0.947 ±15%	0.369 ±18%	0.0566 ±41%
		15	1.624 ±14%	2.683 ±14%	0.996 ±16%	0.402 ±20%
		21	2.900 ±14%	4.936 ±14%	1.705 ±16%	0.751 ±18%
		30	4.026 ±15%	6.879 ±14%	2.388 ±17%	1.220 ±29%
		40	5.603 ±14%	9.165 ±14%	3.107 ±19%	1.404 ±29%
	^{3}He	9	0.0328±14%	0.0533±13%	0.0168±20%	0.00689±33%
		18	0.207 ±14%	0.361 ±13%	0.130 ±18%	0.0389 ±21%
		27	0.547 ±13%	0.885 ±13%	0.320 ±17%	0.101 ±19%
		45	1.568 ±13%	2.511 ±13%	0.939 ±16%	0.281 ±17%
		63	2.469 ±13%	4.180 ±13%	1.462 ±16%	0.419 ±17%
Er	p	3 MeV	0.0215±18%	0.0333±16%	.00947±28%	0.00133±150%
		6	0.172 ±16%	0.279 ±14%	0.0808±23%	0.0164 ±54%
		9	0.441 ±18%	0.750 ±14%	0.218 ±26%	0.143 ±42%
		15	1.167 ±15%	2.142 ±14%	0.690 ±21%	0.264 ±29%
		21	2.373 ±15%	3.806 ±14%	1.175 ±21%	0.662 ±26%
		30	3.903 ±17%	5.864 ±16%	2.029 ±25%	0.654 ±31%
		40	4.741 ±15%	8.147 ±14%	2.567 ±23%	0.896 ±26%
	^{3}He	9	0.0238±15%	0.0427±15%	0.0145±22%	0.0106 ±27%
		18	0.161 ±14%	0.274 ±14%	0.0898±16%	0.0325 ±19%
		27	0.442 ±13%	0.715 ±14%	0.246 ±17%	0.0845 ±19%
		45	1.257 ±13%	2.005 ±14%	0.710 ±17%	0.235 ±18%
		63	2.020 ±14%	3.431 ±14%	1.234 ±17%	0.429 ±18%
Lu	p	3 MeV	0.0122±22%	0.0228±19%	.00664±41%	0.00113±150%
		6	0.0808±27%	0.191 ±20%	0.0458±42%	0.0222 ±150%
		9	0.250 ±19%	0.596 ±15%	0.237 ±24%	0.0223 ±170%
		15	0.908 ±15%	1.772 ±14%	0.494 ±18%	0.226 ±19%
		21	1.700 ±15%	2.881 ±14%	1.036 ±18%	0.491 ±18%
		30	2.494 ±15%	4.539 ±14%	1.617 ±18%	0.785 ±18%
		40	3.427 ±15%	6.297 ±14%	2.181 ±18%	0.784 ±19%
	^{3}He	9	0.0141±23%	0.0273±20%	-	-
		18	0.1003±14%	0.189 ±14%	0.0744±22%	0.0304 ±31%
		27	0.306 ±13%	0.530 ±14%	0.187 ±20%	0.105 ±22%
		45	0.836 ±13%	1.513 ±14%	0.561 ±19%	0.155 ±22%
		63	1.443 ±13%	2.733 ±14%	0.890 ±19%	0.297 ±24%

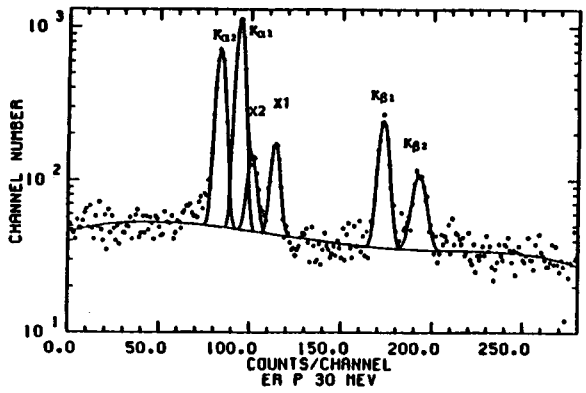

Fig. 1. K-X ray spectrum of Er produced by proton 30 MeV bombardment. Each lines are separated by a least-square fitting assuming Gaussian shapes and 5-th order polynomial.

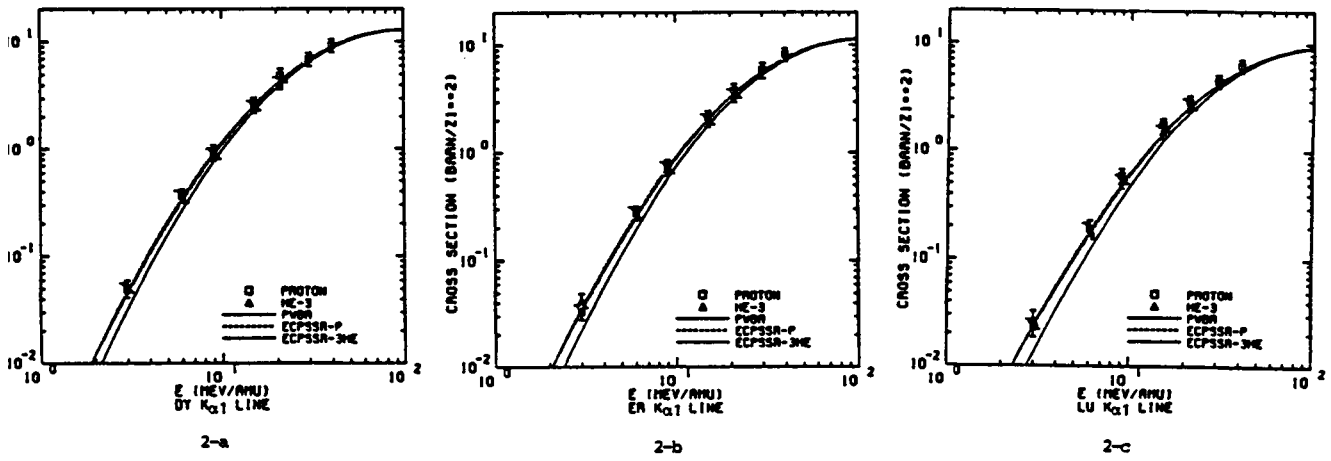

2-a 2-b 2-c

Figs. 2a-c. $K\alpha_1$-X ray production cross sections for Dy, Er and Lu elements. Solid line represents the prediction of the PWBA theory, dashed line for the ECPSSR theory (Proton) and dot and dashed line for the ECPSSR theory (^{3}He), where the values of Ref. 5) and 6) are used as fluorescence yields and radiative widths.

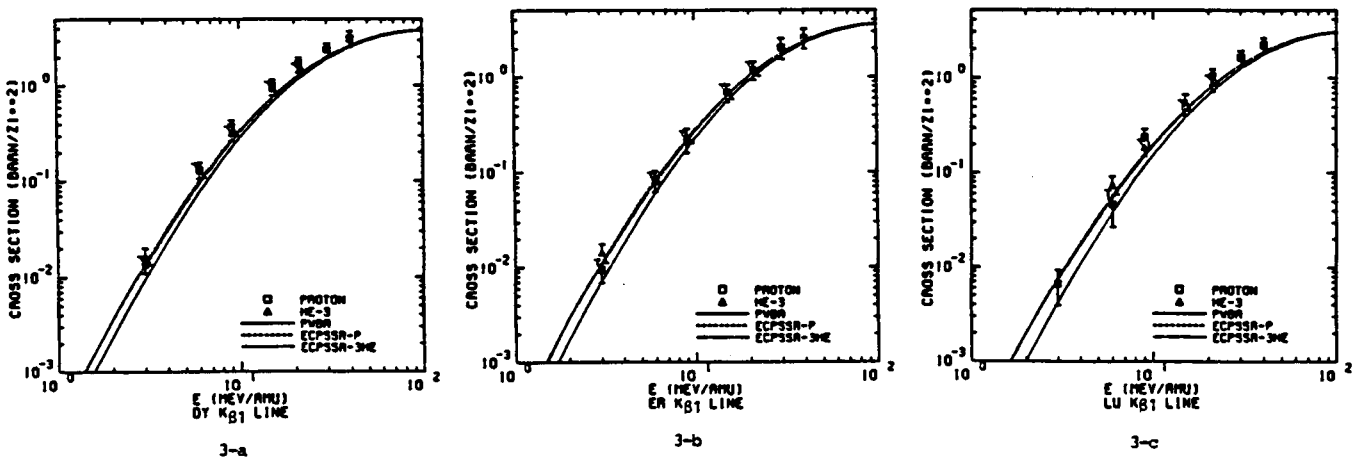

Figs. 3a-c. Same as Fig. 2 except for $K\beta_1$.

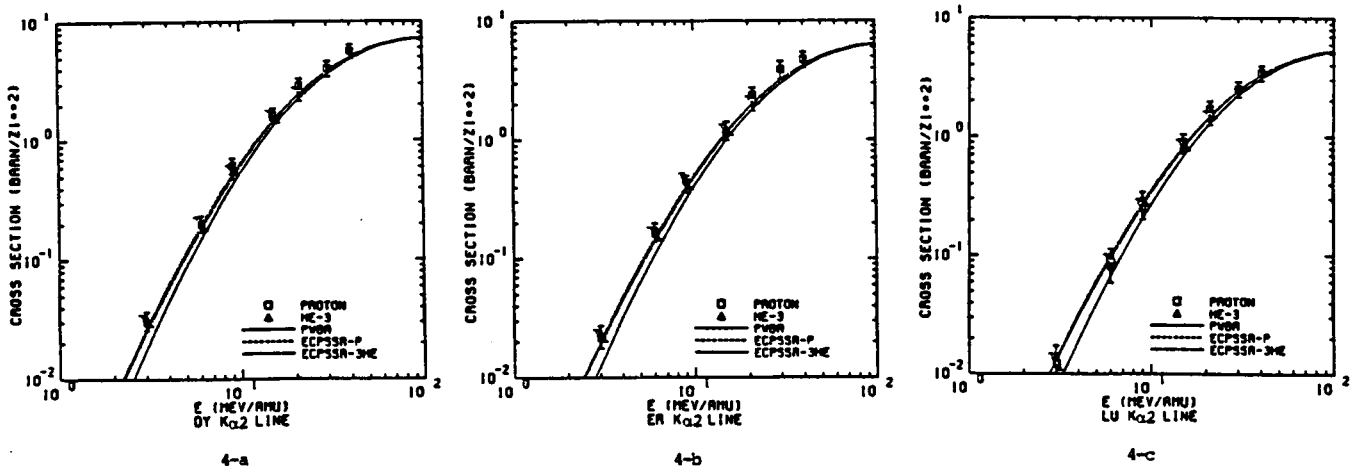

Figs. 4a-c. Same as Fig. 2 except for $K\alpha_2$.

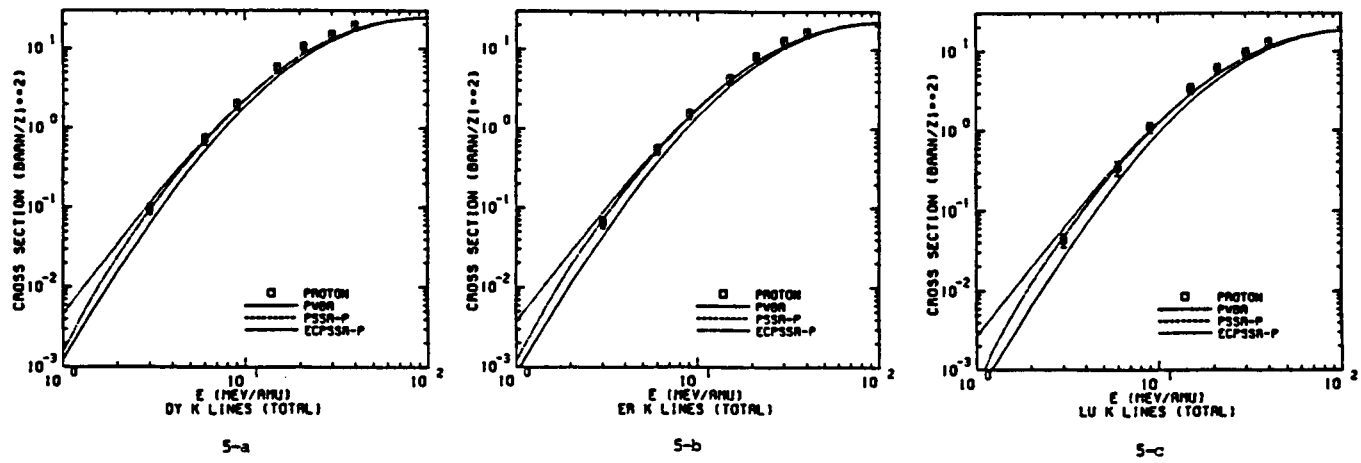

Figs. 5a-c. Total K-X ray production cross sections for proton impact. Solid line represents the prediction of the PWBA theory, dashed line for the PSSR theory (Proton) and dot and dashed line for the ECPSSR theory (Proton).